EPSC Abstracts
Vol. 10, EPSC2015-59, 2015
European Planetary Science Congress 2015
© Author(s) 2015

Magmatic intrusions in the lunar crust

C. Michaut and C. Thorey
Université Paris Diderot, Sorbonne Paris Cité, Institut de Physique du Globe de Paris, F-75013 Paris, France, michaut@ipgp.fr

Abstract

The lunar highlands are very old, with ages covering a timespan between 4.5 to 4.2 Gyr, and probably formed by flotation of light plagioclase minerals on top of the lunar magma ocean. The lunar crust provides thus an invaluable evidence of the geological and magmatic processes occurring in the first times of the terrestrial planets history.

According to the last estimates from the GRAIL mission, the lunar primary crust is particularly light and relatively thick [1] This low-density crust acted as a barrier for the dense primary mantle melts. This is particularly evident in the fact that subsequent mare basalts erupted primarily within large impact basin: at least part of the crust must have been removed for the magma to reach the surface. However, the trajectory of the magma from the mantle to the surface is unknown.

Using a model of magma emplacement below an elastic overlying layer with a flexural wavelength Λ, we characterize the surface deformations induced by the presence of shallow magmatic intrusions. We demonstrate that, depending on its size, the intrusion can show two different shapes: a bell shape when its radius is smaller than 4 times Λ or a flat top with small bended edges if its radius is larger than 4 times Λ [2]. These characteristic shapes for the intrusion result in characteristic deformations at the surface that also depend on the topography of the layer overlying the intrusion [3].

Using this model we provide evidence of the presence of intrusions within the crust of the Moon as surface deformations in the form of low-slope lunar domes and floor-fractured craters. All these geological features have morphologies consistent with models of magma spreading at depth and deforming an overlying elastic layer.

Furthermore, at floor-fractured craters, the deformation is contained within the crater interior, suggesting that the overpressure at the origin of magma ascent and intrusion was less than the pressure due to the weight of the crust removed by impact [3]. The pressure release due to material removal by impact is significant over a depth equivalent to the crater radius. Because many of these floor-fractured craters are relatively small, i.e. less than 20 to 30 km in radius, this observation suggests that the magma at the origin of the intrusion was already stored within or just below the crust, in deeper intrusions.

Thus, a large fraction of the mantle melt might have been stored at depth below or within the light primary crust before reaching shallower layers. This, in turn, should have influenced the thermal and geological evolution of this crust.

Acknowledgements

This work has been supported by the UnivEarths LabEx program of Université Paris Diderot, Sorbonne Paris Cité (ANR-10-LABX-0023 and ANR-11-IDEX-0005-02) and by PNP/INSU/CNES.

References

[1] Wieczorek, M., et al, The crust of the Moon as seen by GRAIL, Science 339, 671-675, 2013.

[2] Michaut, C. Dynamics of magmatic intrusions in the upper crust : Theory and applications to laccoliths on Earth and the Moon, J. Geophys. Res. 116, doi:10.1029/2010/JB008108, 2011.

[3] Thorey, C., and C. Michaut, A model for the dynamics of crater-centered intrusions: Application to lunar floor-fractured craters. J. Geophys. Res. Planets, 119(1):286–312, January 2014.

EPSC Abstracts
Vol. 10, EPSC2015-71, 2015
European Planetary Science Congress 2015
© Author(s) 2015

Highest volcanoes on terrestrial planets and dwarf-planets adorn the deepest depressions of their respective bodies

G.G. Kochemasov; IGEM of the Russian Academy of Sciences, kochhem.36@mail.ru

Four highest volcanoes of the inner solar system tower above four largest and deepest hemispheric depressions of the Earth, Moon, Mars, and Vesta. Of course, this is not a mere coincidence; behind of this fundamental fact stays an equally fundamental planetary regulation. The wave planetology based on elliptical keplerian orbits of cosmic bodies evoking their wave warping shows that the fundamental wave 1 inevitably produces hemispheric tectonic dichotomy. One hemisphere rises, the opposite falls. The uprising half increases its planetary radius and space and thus is intensively cut by numerous faults and rifts. The antipodean subsiding half decreases its radius and space and thus is intensively compacted and affected by folds and faults. Forming extra material finds its way out in form of volcanic ridges and volcanoes. The strongest compaction caused by the wave 1 subsidence produces most voluminous eruptions. That is why the relation exists between the largest and deepest hemispheric basins and the highest basic volcanoes having mantle roots [1-4]. On the Earth's Pacific Ocean floor stay the Hawaiian volcanoes; on the lunar Procellarum Ocean occurs Crater Copernicus (erroneously taken as an impact feature); Martian Vastitas Borealis is adorned with Olympus Mons; Vestan Reasilvia Basin (obviously tectonic not impact feature) has the central mountain – the highest volcanic peak in the Solar system (Fig. 1-4). A regular row of increasing heights of these largest volcanoes extends in the outward direction.

A study of the dwarf-planet Ceres only begins (DAWN project). Already the first distant images of this globe about 950 km in diameter have shown that it is, as was predicted [5], tectonically two-faced or dichotomous body (Fig. 5, 6). It seems that on its relatively even subsided hemisphere there are some elevated locations often bright white in color (Fig. 6). They could represent prominent "edifices" covered with frozen ices – degassing traces [6].

References: [1] Kochemasov G.G. 1993. Relief-forming potential of planets // 18th Russian-American microsymposium on planetology, Abstracts, Oct. 9-10, 1993, Moscow, Vernadsky Inst. (GEOKHI), 27-28. **[2]** Kochemasov G.G. 2009a. A regular row of planetary relief ranges connected with tectonic granulations of celestial bodies // New Concepts in Global Tectonics Newsletter, # 51, 58-61. **[3]** Kochemasov G.G. 2009b. A quantitative geometric model of relief-forming potential in terrestrial planets // EPSC Abstracts, Vol. 4, EPSC2009-16-1. **[4]** Kochemasov G.G. Why four highest volcanoes of the rocky planets adorn their deepest planetary wide depressions: Earth, Mars, Vesta and Moon // NCGT Journal, v. 2, # 4, Dec. 2014, 85-88. **[5]** Kochemasov G.G. From Vesta to Ceres: predicting spectacular dichotomous convexo-concave shape for the largest mini-planet in the main asteroid belt // Vesta in the light of Dawn: first exploration of a protoplanet in the Asteroid Belt, Febr. 3-4, 2014, Houston, Texas, LPI Contribution # 1773, Abstract # 2003. pdf. **[6]** Kochemasov G.G. Ceres' two-face nature: expressive success of the wave planetology // NCGT Journal, v. 3, #1, March 2015, 63-64.

Fig. 1. Mauna Kea

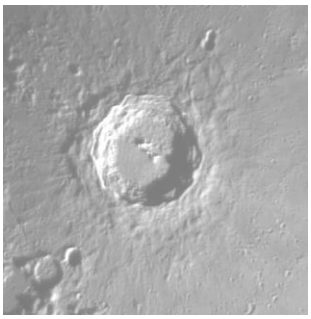

Fig. 2. Crater Copernicus, Moon

Fig. 3. Olympus Mons, Mars.

Fig. 4. Central peak of Rheasilvia, Vesta

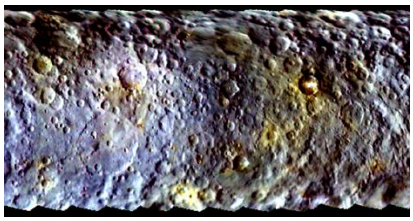

Fig. 5. Ceres' topography. Pia19063.

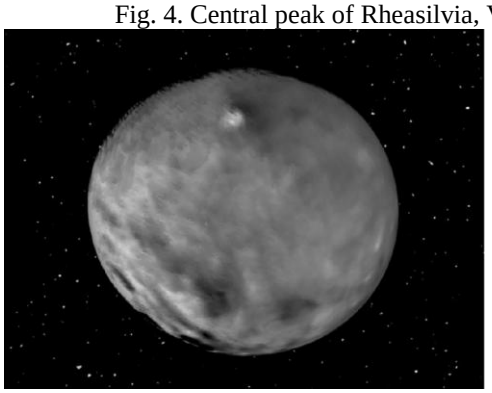

Fig. 6. Ceres, OUBF3CLM.JPG. Distant view

EPSC Abstracts
Vol. 10, EPSC2015-95, 2015
European Planetary Science Congress 2015
© Author(s) 2015

Detection of lunar floor-fractured craters using machine learning methods

C. Thorey
Université Paris Diderot, Sorbonne Paris Cité, Institut de Physique du Globe de Paris, F-75013 Paris, France, thorey@ipgp.fr

Abstract

About 200 Floor Fractured Craters (FFCs) have been identified by Schultz (1976) on the Moon, mainly around the lunar maria. These craters are a class of impact craters that are distinguished by having radially and concentric floor-fractured networks and abnormally shallow floors. In some cases, the uplift of the crater floor can be as large as 50% of the initial crater depth. These impact craters are interpreted to have undergone endogenous deformations after their formation.

The recent theoretical model for the dynamics of crater-centered intrusions of Thorey and Michaut (2014) and recent morphological and geological studies by Jozwiak et al. (2012) showed that intrusion of magma beneath the crater floor is the most plausible scenario to produce the morphological features observed at floor-fractured craters. In addition, taking advantage of the resolution of the lunar gravity field obtained from the NASA's Gravity Recovery and Interior Laboratory (GRAIL) mission, in combination with topographic data obtained from the Lunar Orbiter Laser Altimeter (LOLA) instrument, Thorey et al. (2015) showed that their gravitational signatures are also consistent with the intrusion of large volumes of magma below their floors.

Recent estimate from the GRAIL mission confirms the relatively low density of the lunar crust (Wieczorek et al., 2013). Given the large density of the melt inferred from the composition of the mare basalts (Wieczorek et al., 2001), the volume of intruded mantle melt into the lunar crust might be large. Identifying potential sites for magmatic intrusions is important to understand the thermal and magmatic evolution of the Moon. In addition, these shallow magmatic reservoirs tell us more about the structure and geological evolution of the lunar crust and the trajectory of the magma.

Herein, we will discuss the possibility of using machine learning algorithms to try to detect new crater-centered intrusions on the Moon among the $\sim$ 60000 craters referenced in the most recent catalogs (Salamuniccar et al., 2014). In particular, we will use the gravity field provided by the GRAIL mission and the topographic dataset obtained from the LOLA instrument to design a set of representative features for each crater. We will then discuss the possibility of designing a binary supervised classifier, based on these features, to discriminate between the presence or absence of a crater-centered intrusion below a specific crater. First predictions from different classifier in terms of their accuracy and uncertainty will be presented.

Acknowledgements

This work is partially funded by the UnivEarths LabEx program of Sorbonne Paris Cité (ANR-10-LABX-0023 and ANR-11-IDEX-0005-02) and by PNP/INSU/CNES.

References

Peter H Schultz. Floor-fractured lunar craters. *The Moon*, 15(3-4):241–273, September 1976.

Clément Thorey and Chloé Michaut. A model for the dynamics of crater-centered intrusion: Application to lunar floor-fractured craters. *J. Geophys. Res. Planets*, 119(1):286–312, January 2014.

Lauren M Jozwiak, James W Head, Maria T Zuber, David E Smith, and Gregory A Neumann. Lunar floor-fractured craters: Classification, distribution, origin and implications for magmatism and shallow crustal structure. *J. Geophys. Res.*, 117(E11): E11005, November 2012.

Clément Thorey, Chloé Michaut, and Mark A Wieczorek. Gravitational signatures of lunar floor-fractured craters (FFC). *Earth and Planetary Science Letters*, *In press*.

Mark A. Wieczorek, G A Neumann, Francis Nimmo, W S Kiefer, G J Taylor, H J Melosh, R J Phillips, S C Solomon, J C Andrews-Hanna, S W Asmar, A S Konopliv, F G Lemoine, D E Smith, M M Watkins, J G Williams, and M T Zuber. The crust of the Moon as seen by GRAIL. *Science*, 339(6120):671–675, February 2013.

Mark A. Wieczorek, M T Zuber, and R J Phillips. The role of magma buoyancy on the eruption of lunar basalts. *Earth and Planetary Science Letters*, 185 (1-2):71–83, 2001.

Goran Salamuniccar, Sven Lončarić, Arne Grumpe, and Christian Wöhler. Hybrid method for crater detection based on topography reconstruction from optical images and the new LU78287GT catalogue of Lunar impact craters. *Advances in Space Research*, 53(12):1783–1797, June 2014.

EPSC Abstracts
Vol. 10, EPSC2015-99, 2015
European Planetary Science Congress 2015
© Author(s) 2015

A Field of Small Pitted Cones on the Floor of Coprates Chasma: Volcanism inside Valles Marineris

E. Hauber[(1)], **P. Brož** [(2,3)], A. P. Rossi[(4)] and G. Michael[(5)]
(1) Institute of Planetary Research, DLR, Berlin, Germany (2) Institute of Geophysics ASCR, v.v.i., Prague, Czech Republic, Petr.broz@ig.cas.cz (3) Institute of Petrology and Structural Geology, Charles University in Prague, Czech Republic (4) Jacobs University Bremen, Bremen, Germany (5) Freie Universität Berlin, Germany.

Abstract

We present observations of a field of >100 pitted cones and mounds situated on the floor of Coprates Chasma (part of Valles Marineris (VM); Fig. 1), which display similarities to terrestrial and martian scoria cones. If these cones are indeed volcanic in origin, they will significantly expand our knowledge about the morphometry of pyroclastic cones on Mars. Moreover, a magmatic origin, which would necessarily post-date the opening of the main VM troughs, would contribute to our understanding of the volcano-tectonic evolution of VM.

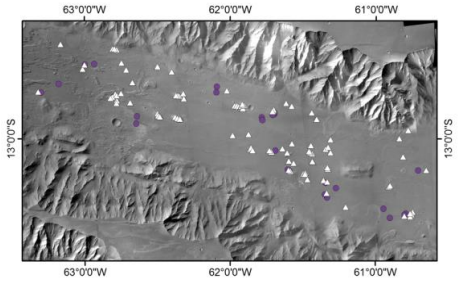

Figure 1: Location of investigated cones (triangles) and mounds (circles) in eastern Coprates Chasma (CTX mosaic). The edifices are spread over the entire trough.

1. Introduction

It has long been suggested that volcanism played a role in the formation of Valles Marineris [e.g., 1], but unambiguous evidence has been rare. Recent images acquired by the CTX camera (~5-6 m/px) reveal the existence of several fields of small pitted cones, mainly associated with chaotic terrain in the eastern part of Valles Marineris [2,3] and also in Coprates Chasma [3,4]. Coprates Chasma is a linear graben extending in west-east direction for ~1000 km. It probably formed as one of the most recent main depressions of the VM system. Based on morphological similarities, Harrison [3] suggested that these cones might represent scoria cones, but without providing further details. Meanwhile the whole area is covered by CTX images that enable analysis of the entire cone field. One cluster of pitted cones is covered by a HiRISE stereo pair, allowing the production of a HiRISE Digital Elevation Model (DEM). Based on these new data, we studied the cones in unprecedented detail. Here we show preliminary results.

2. Data and methods

We used images from CTX, HRSC, and HiRISE. Topographic information is derived from single MOLA shots, HRSC DEMs, and HiRISE and CTX DEMs that were computed using the methods described in [5]. HiRISE and CTX DEMs have a grid spacing of ~1 m/pixel and ~10 m/pixel and a vertical accuracy of approximately a few decimeters and a few meters, respectively.

3. Observations

The cones and mounds are widely spread over a total area of about 155 × 35 km. Some cones stand alone, others are concentrated in clusters with up to ten edifices. In plan view, their morphology is characterized by circular to elongated shapes. Their flanks have slopes up to 25°, but are generally more shallow. Cone basal diameters vary from 0.5 km up to 2.2 km, with a mean of 1 km (based on 23 cones). Most of them have summit craters (Fig. 2a), which have diameters from 0.15 km up to 0.8 km (mean 0.3 km). In some cases craters are superposed by other craters suggesting the lateral migration of explosion sites or feeder dikes. Typically, the cones are not breached, but there are two exceptions which seem to result from explosion and/or collapse of the cone. In some cases cones are superposed on units with a rough texture that forms local bulges (Fig. 2a). To compare the cones morphologically with martian and terrestrial analogues, we measured the basal diameters of the cones (W_{CO}) and the crater diameters (W_{CR}). The W_{CR}/W_{CO} ratio ranges between 0.22 and 0.5, with an average of 0.34. Fresh terrestrial and Martian scoria cones have ratios of ~0.4 [6], and ~0.27 [7], respectively. The cones appear relatively pristine, and small impact craters do not change their shapes significantly.

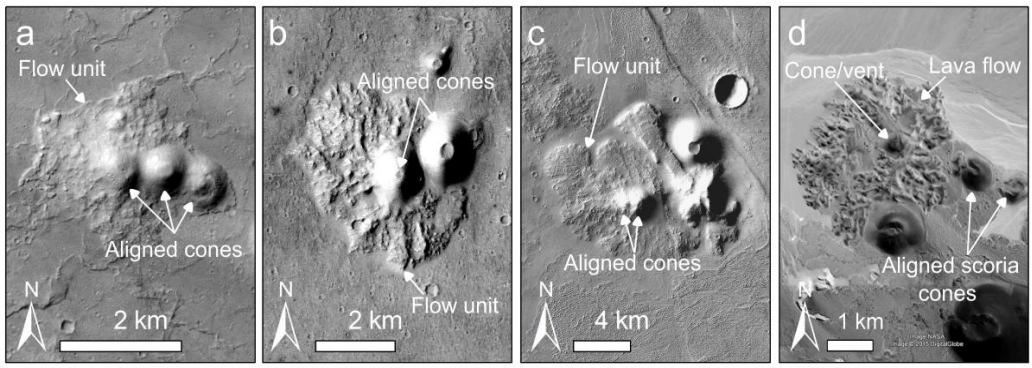

Figure 2: Cluster of investigated cones in Coprates Chasma (a) and comparison to similar features on Mars and Earth (b-d). (a) HiRISE ESP 034131 1670, centered 12.73°S, 62.8°W, (b) Hydraotes Chasma; CTX image G19_025493_1800, 0.2°N, 33.83°W, (c) Ulysses Colles; CTX image G11_022582_1863, 5.81°N, 122.59°W, (d) Andes (Earth); NASA, Digital Globe, Google Earth™, 26.29°S, 67.35°W.

4. Summary and Conclusions

The studied cones bear many morphological similarities to edifices in Hydraotes Colles [2] (Fig. 2b) and Ulysses Colles [7] (Fig. 2c) that were previously interpreted as scoria cones and with terrestrial scoria cones (Fig. 2d). The Coprates cones are smaller (WCO on average 1 km) than the Hydraotes cones (1.5 km) and the Ulysses cones (2.3 km), but with similar WCR/WCO ratios (0.34 for cones in Coprates and 0.27 for cones in Ulysses). This might be caused by a higher atmospheric pressure at the floor of Coprates Chasma (~5 km beneath Mars' global datum) disabling a wider dispersion of ejected particles from the vent [8], by a smaller amount of erupted material or by smaller erosion. The associated elevated rough units around the edifices are similar to what is observed in Hydraotes Colles and Ulysses Colles. Similar rough textures around terrestrial scoria cones are associated with lava flows and possibly pyroclastic deposits.

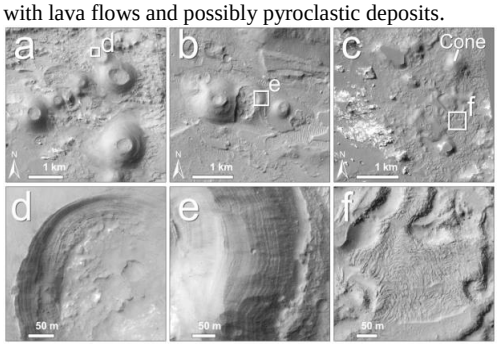

Figure 3: Details of cone morphology. (a) ESP_033986_1670, 12.73°S/297.2°E. (b) ESP_036109_1675, 12.4°S/297.21°E. (c) ESP_036-254_1665, 13.28°S/298.52°E. (d) Parallel, flat-lying layers exposed in inner crater wall. (e) Similar fine layering in scarp of eroded cone. (f) Exhumed (?) surface adjacent to cone, reminiscent of a lava flow surface texture.

At HiRISE resolution, further details provide possible hints to the nature of the cones. Where scarps break the surface of the otherwise smooth-textured cones, series of fine parallel layers are visible in some places (Fig. 3 a and d, b and e). Although other interpretations are possible, this would be consistent with a volcanic origin of some cones, specifically as phreatomagmatic edifices, e.g., tuff cones. In another location, the surface texture near a cone is reminiscent of a lava flow (Fig. 3 c and f). The spatial distribution of cones (2 point-azimuth analysis; for details see ref [9]) reveals two main trends of a possible structural control. One is oriented parallel to the main VM trend (~N110°), while another is ~N75°. The first trend suggests that magma feeding the cones may have ascended (as dikes?) along weakness zones created by VM formation. Preliminary age determinations based on crater counting suggest that the cones were formed at 200 Ma to 400 Ma.

Our preliminary results, therefore, support previous suggestions [3,4] that this field is probable volcanic in origin and consists primarily of scoria cones. Ongoing investigations will help to assess alternative formation scenarios (e.g., mud volcanism), extend our knowledge on scoria cone formation on Mars and will also help to provide further insight about the evolution of Valles Marineris.

Acknowledgements: This study was partly supported by the Grant 580313 of the program of the Charles University Science Foundation GAUK.

References: [1] Lucchitta, B.K. (1987) Science, 235, 565-567. [2] Meresse, S. et al. (2008) Icarus, 194, 487–500. [3] Harrison, T.N. (2012) LPSC, XLIII, Abstract #1057. [4] Harrison, K.P. and Chapman, M.G. (2008) Icarus, 198, 351–364. [5] Moratto, Z.M. et al. (2010) LPSC, XLI, Abstract #2364. [6] Wood, C.A. (1980) J. Volcanol. Geotherm. Res., 7, 387–413. [7] Brož, P. and Hauber, E. (2012) Icarus, 218, 1, 88–99. [8] Brož, P. et al. (2014) Earth Planet. Sci. Lett., 406, 14-23. [9] Brož, P. and Hauber, E. (2013) JGR-Planets, 118, 1656-1675.

EPSC Abstracts
Vol. 10, EPSC2015-255, 2015
European Planetary Science Congress 2015
© Author(s) 2015

Paleotectonism in the Noachis-Sabaea region, Southern Highlands of Mars; Preliminary Modelling and Reconstruction of Events

T. Ruj (1, 2), G. Komatsu (1, 2), J. M. Dohm (3), H. Miyamoto (3), F. Salese (1, 2, 4).

(1) International Research School of Planetary Sciences, Università d'Annunzio, Viale Pindaro 42, 65127 Pescara, Italy
(2) Dipartimento di Ingegneria e Geologia, Università d'Annunzio, Italy
(3) The University Museum, University of Tokyo, Hongo 7-3-1, Bunkyo-ku, Tokyo 113-0033, Japan
(4) INAF-Istituto Nazionale di Astrofisica, Osservatorio Astronomico di Teramo, Italy
(trishit@irsps.unich.it)

1. Introduction. Paleotectonism of Mars has been investigated at global to local scales [1], with particular focus on Tharsis and its components [1], [2]. Such examples include the southern and eastern margins of the Thaumasia plateau, namely the Thaumasia highlands and Coprates rise mountain ranges respectively [3], and structurally-controlled basins and associated highly-degraded massifs that are interpreted to be volcanoes such as in the extremely ancient provinces like Terra Sirenum [4] and Terra Cimmeria [5].

This is the first geologic investigation with the primary purpose of determining the paleotectonic history of the Terra Sabaea and eastern Noachis Terra region (referred here as the Noachis-Sabaea region), including faults and wrinkle ridges located to the northwest of the Hellas impact basin. Though, there have been mapping investigations, which have revealed: the general geologic history of the region such as those based on Viking data [6], centres of tectonic activity in the eastern equatorial region, including the Isidis/Syrtis Major volcanic province and Arabia Terra [1], and an investigation which resulted in the identification of macrostructures (faults with lengths exceeding 1,000 km) which transect the region with respect to Mars Global Surveyor (MGS) Mars Orbiter Laser Altimeter (MOLA), gravity, and paleomagnetic data [7].

In this on-going investigation, we are identifying, characterizing, and mapping lineaments and scarps, which we interpret to be both tectonically derived and non-tectonic features. Tectonic features include those that formed prior to the Hellas impact event and non-tectonic features are those related to the Hellas impact event and modified by Hellas impact. We are using MOLA global colorized elevation map (Fig. 1), HRSC and CTX images and stratigraphic information of the newly published global geologic map of Mars [8]. Here, we present our preliminary map, containing information which will be used to unravel the complex paleotectonic history of the Noachis-Sabaea region, including pre-Hellas, Hellas-impact, and post-Hellas deformation.

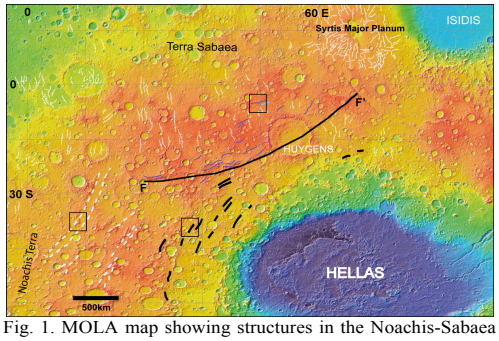

Fig. 1. MOLA map showing structures in the Noachis-Sabaea region, including three sets of grabens (set 1 indicated by bold black lines, set 2 by white dotted lines, and set 3 by purple lines). Wrinkle ridges (narrow white lines) and grabens (FF'-curvilinear black line) are also shown. Black rectangular boxes are zoomed in Fig. 2.

2. Structural observation of the area. Deformation of the Noachis-Sabaea region includes three distinct sets of graben, determined through their orientations and morphologic and topographic expressions. The set-1 grabens (Fig. 2a) are mainly concentric to the Hellas basin and may have formed due to the Hellas impact event, including stress relaxation of impact energy (hoop stress) [9]. Of the three sets, this set of grabens are the shortest in length.

Set-2 grabens (Fig. 2b) have NNE-SSW to N-S trends, with the largest one having a length and width of ~1200 km and ~80 km, respectively. These grabens, which have corrugated boundaries, contain a remnant crustal basement. Both the horst and graben have been significantly modified by wind, water and gravity-driven processes and the graben being partly infilled by sediments. In addition, Late Noachian flood volcanism has been reported to have sourced from several of the graben floors [10]. Importantly, more detailed analysis is necessary to determine whether the formation of these grabens, including their geometric patterns, were influenced by impact craters, including those buried [11]

and/or possibly basement structures no longer visible at the Martian surface.

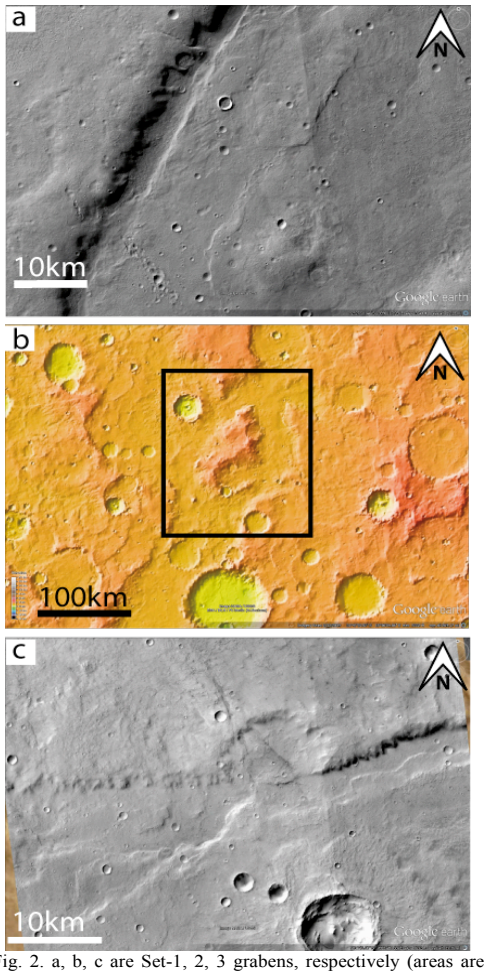

Fig. 2. a, b, c are Set-1, 2, 3 grabens, respectively (areas are marked in the Fig. 1). Fig. 2a is a CTX image and shows a half graben structure, and Fig. 2b is MOLA colourised elevation map showing a ridge-like structure within the graben (marked with rectangle). Fig. 2c is a typical shape of grabens shown in a CTX image.

Set-3 grabens (Fig. 2c) are concentrated mainly in the Terra-Sabaea part of the study region having NE-SW to E-W trends. These grabens are not extended when compared to the set-2 grabens; they are smaller in extension but form a graben network that collectively extends up to 2800 km. The Huygens impact event appears to post-date the formation of most of the grabens (based on the stratigraphic and crosscutting relations among the grabens and Huygens impact crater materials). Though, there is a ridge-like structure that deforms the central part of the Huygens basin, which marks either reactivation of a pre-existing basement structure or post-impact deformation including contraction. In addition, the northwest rim appears to be deformed. These grabens appear to terminate northeast of Huygens near the southern margin of the Syrtis Major volcanic province and a large curvilinear scarp which could mark the highly degraded rim of the Isidis impact basin rim and to the west near the longest graben of the set-2 grabens. Identification, mapping, and characterizing such details will help to unravel the paleotectonic history in the region.

3. Discussion. Our preliminary mapping in the Noachis-Sabaea region indicate several modes of origin of the tectonic structures, some are not necessarily tied to the Hellas impact event. The Hellas impact event, estimated to have occurred at ~4.0 Ga [12], for example, likely contributed to set-1 grabens, including stress relaxation following the impact event. But what about the other system of structures? There are multiple possible contributors to the present-day strain in addition to the Hellas impact event that must be thoughtfully considered. Possible contributors include the putative Arabia Terra impact [13] and the putative Utopia impact [14], the Isidis impact event and activity related to the development of the Syrtis Major volcanic province [1], and possible plate tectonism such as reported for the Terra Meridiani region of Mars [15]. The latter is of particular interest, as there is more and more evidence for an ancient dynamic Mars recorded possibly in a felsic basement [16]. Also, there has been felsic rocks [17], interpreted to be granite, in the region. Thus could the processes that resulted in the formation of some of the fault systems (e.g., set 2 and 3, and F-F') be related to the possible granite rocks, or could the felsic rocks be indicative of an ancient southern highlands basement which records dynamic activity? We will present the paleotectonic information with main focus mainly on the tectonic fabrics and their origins at the conference providing working hypotheses to help explain the mapping results.

References: [1] Anderson, R. C. et al., 2008a, *Icarus, 195*, 537-546. [2] Anderson, R. C. et al., 2001a, *JGR, 106, E9*, 20563-20585. [3] Dohm, J. M. et al., 2001b, *U.S.G.S. Map I-2650* at 1:5,000,000 scale. [4] Anderson, R. C. et al., 2012, *43rd LPSC*, Abstract #2803. [5] Fairén, A. G. et al., 2002, *Icarus, 160*, 220-223. [6] Greeley, R. and Guest, J. E., 1987, *U.S.G.S. Map I-1802B* at 1:15,000,000 scale. [7] Dohm, J. M. et al., 2002, *LPSC, XXXIII*, Abstract #1639. [8] Tanaka, K. L. et al., 2014, *U.S.G.S. Scientific Investigations Map* 3292. [9] Wichman, R. W. et al., 1989, *JGR Solid Earth, 94, B12*, 17333-17357. [10] Rogers, A. D. and Nazarian, A. H., 2013, *JGR Planets, 118*, 1094-1113. [11] Rodriguez, J. A. P. et al., 2005b, *JGR, 110*, E06003. [12] Werner, S. C., 2009, *Icarus, 201*, 44-68. [13] Dohm, J. M. et al., 2007a, *Icarus, 190*, 74-92. [14] McGill, G.E., 1989, *JGR, 94*, 2753-2759. [15] Connerney, J. E. P. et al., 2005, *PNAS, 102*, 14970-14975. [16] Dohm, J. M. et al., 2015, *46th LPSC*, Abstract #1741. [17] Wrey, J. J. et al., 2013, *Nature Geoscience, 6*, 1013-1017.

EPSC Abstracts
Vol. 10, EPSC2015-296, 2015
European Planetary Science Congress 2015
© Author(s) 2015

Fluvial channels in the north-western part of Noachis Terra, Mars: Implications for tectonic controls

K. De (1), N. Dasgupta (2), A. Kundu (1) and P. Chauhan (3)
(1) Asutosh College, Kolkata, India (2) Presidency University, Kolkata, India, (3) Space Application Centre (ISRO), Ahmedabad, India (de.keyur@gmail.com)

Abstract

Palaeochannels in the western part of Noachis Terra are mapped to understand their origin and also the control on their courses. Relation to impact craters, trends and cross-correlations between their paths indicates to impact-related origin and tectonic lineament controlled courses for the rivers.

1. Introduction

Fluvial channels are reported from Martian surface long ago, yet their origin and evolution are still not very clear [1]. In general the source of Martian valley networks are ascribed to groundwater sapping process, though hypotheses suggesting subsurface ice melting and rainwater are also proposed [1]. Presently available high resolution images like MOC, HiRISE, HRSC, CTX help to identify many paleochannels with complex drainage history. Terrestrial analogs of these channels help scientists to understand the origin of Martian valley networks and the processes responsible for their evolution. Martian streams indicate considerable degree of surface incision though it is lesser than that on Earth. Martian low-order river valleys often have relatively flat longitudinal profile when compared to terrestrial valleys [1]. There are evidences that the erosive action of these fluvial channels were promoted by rainfall. Our study aim to find the source of river water and the control over their courses in the north-western part of Noachis Terra, a region that is still geologically less explained compared to the other regions of the red planet [2, 3, 4].

2. Channel configuration and correlation

In the north-western part of Noachis Terra, within an area [29˚W, 26˚S to 19˚W, 32˚S] (Figure 1) of 164500sqkm, palaeochannels display a specific pattern or orientation. A detailed study of the topographic features and the channels reveal that the channel courses were possibly controlled by tectonic lineaments. The area displays sinuous river channels with prominent trend of N-S to NNE-SSW. In the area of study, there are a series of grabens with consistent E-W trend [5]. All N-S trending fluvial channels terminate at these grabens almost at right angles (Figure 1). Consistent orientation of these channels for considerably (30-50km) long stretches invites to think over the control on such a straight

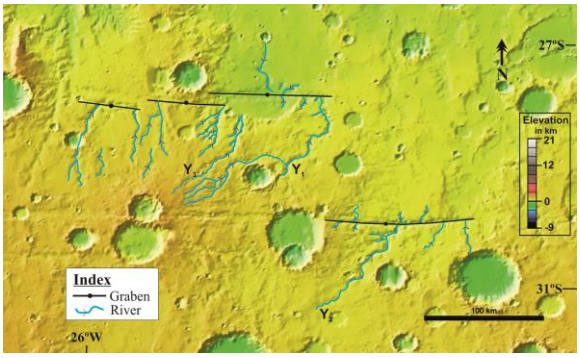

Figure 1: MOLA [6] colourised elevation map of the area of study in the north-western part of Noachis Terra. Note that the rivers emerge from impact crater rim or periphery of impact crater ejecta blanket.

course. MOLA [6] based profiles along different E-W sections across the palaeochannels show that the levels of exposed ground on eastern and western banks are almost at same altitude. Therefore, the linear depressions which were followed by these channels possibly are extensional fractures, without any relative vertical displacement across them, rather than normal faults leading to crustal extension. Moreover most of the N-S trending channels emerge from the impact-crater rims or from the periphery of ejecta blankets (Figure 1). This fact leads to a proposition that the source of water that created the channels was sub-surface ice that melted due to the

impacts of bolides. Segments of the N-S palaeochannels and also the tributaries follow E-W trend at parts, possibly controlled by the set of fractures similar in trend to that of grabens. Therefore, altogether the N-S trending palaeochannels and E-W trending tributary channels reflect a rectangular drainage pattern commonly found in regions with perpendicular joint set [7]. A statistical analysis on the palaeochannels has been done to examine the structural control behind the river courses. Correlated paths of three rivers (Y_1=120km, Y_2=90km, Y_3=140km, Figure 1), show high cross-correlation coefficients [8] (ranging from 0.5 to 0.98) (Figure 2,3)

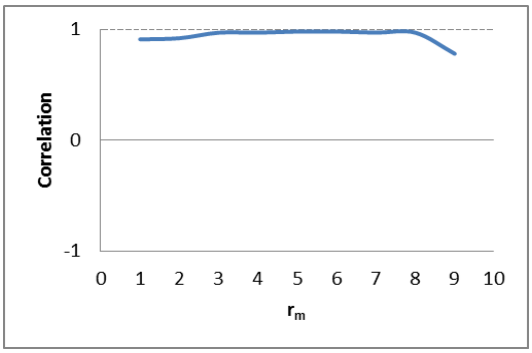

Figure 2: Correlation graph between River Y_1 and Y_2 of Figure 1.

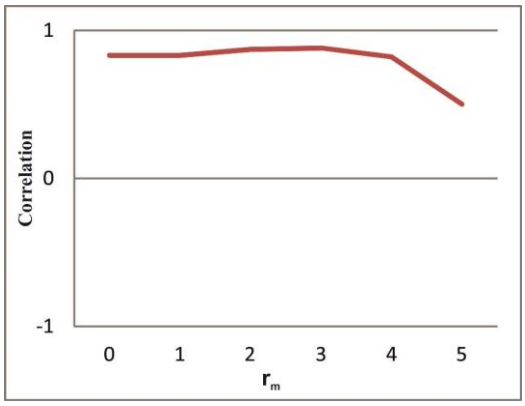

Figure 3: Correlation graph between River Y_1 and Y_3 of Figure 1.

implying a striking similarity between the river courses, few tens of kilometers apart from each other, within the area. We propose that such systematic similarities in their courses are due to tectonic controls, which here possibly were N-S trending and E-W trending fracture systems. The river channels are guided by these fracture systems that have developed in the area and not merely by the topography of the area.

3. Conclusions

Palaeochannels in the western part of Noachis Terra exhibiting a general N-S trend emerge either from the rims of impact craters or from the margins of ejecta blankets revealing their origin from subsurface ice that melted by the bolide impacts. The N-S trending palaeochannels along with their E-W trending segments and palaeotributaries indicate to a tectonic control on their courses. High values of cross-correlation coefficients indicate similarities between the channel courses which is only possible if the channels followed tectonic lineaments.

Acknowledgement

The authors acknowledge a project grant from the Space Applications Centre (ISRO), Ahmedabad, India.

References

[1] The Geology of Mars: Evidence from Earth-Based Analogs, Edited by M. G. Chapman, Cambridge University Press, 2007.

[2] Aittola, M., Korteniemi, J., Öhman, T., Törmänen, T. and Raitala, J.: Geology of Central Noachis Terra, Mars Proceeding Lunar and Planetary Science Conference, 38, 1654, 2006.

[3] Korteniemi, J., Aittola, M., Öhman, T., Törmänen, T. and Raitala, J.: Water and ice in central Noachis Terra, Mars?, 42nd Vernadsky-Brown Microsymposium on Comparative Planetology , Moscow, Russia, 2005.

[4] Raitala, J., Aittola, M., Korteniemi, J., Öhman, T. and Törmänen, T.: A Pingo Group on Noachis Terra, Mars, 50th Vernadsky-Brown Microsymposium on Comparative Planetology, Moscow, Russia, 2009.

[5] De, K., Kundu, A., Chauhan, P. and Dasgupta, N.: An example of consistent palaeostress regime resulting in morphometric irregularity in the north-western part of Noachis Terra, Mars, (accepted), Current Science.

[6] Smith, D., Neumann, G., Arvidson, R. E., Guinness, E. A. and Slavney, S., Mars Global Surveyor Laser Altimeter Mission Experiment Gridded Data Record. NASA Planetary Data System, MGS-M-MOLA-5-MEGDR-L3-V1.0, 2003.

[7] Monroe, J. and Wicander, R.: The Changing Earth: Exploring Geology and Evolution, 7th Edition, Cengage Learning, 2014.

[8] Davis, J., C.: Statistics and Data Analysis in Geology, 3rd Edition, John Wiley & Sons, 2002.

EPSC Abstracts
Vol. 10, EPSC2015-304, 2015
European Planetary Science Congress 2015
© Author(s) 2015

Tectonism and Magmatism on Asteroids

D. L. Buczkowski (1) and D. Y. Wyrick (2)
(1) Johns Hopkins University Applied Physics Laboratory, Laurel, Maryland, USA (Debra.Buczkowski@jhuapl.edu); (2) Southwest Research Institute, San Antonio, Texas, USA .

Abstract

Linear features generally accepted as tectonic structures have been observed on several asteroids and their presence has implications for the internal structure, strength and evolution of these various bodies. Observations of several small bodies have identified different physical mechanisms by which linear features can be formed. Analysis shows that asteroid lineaments appear to have different origins. We also discuss the potential for volcanism and/or magmatism on asteroids, especially in regard to Vesta which, as a differentiated proto-planet, is a unique body with which to study the role that internal rheologies and structures play on surface features.

1. Introduction

We present a review of the solar system asteroids that have been visited by spacecraft—951 Gaspra, 243 Ida, 253 Mathilde, 433 Eros, 25143 Itokawa, 2867 Steins, 5535 Annefrank, 21 Lutetia and 4 Vesta—and discuss how analyses of linear structures observed on these small terrestrial bodies have implications for the tectonics of asteroids, models of linear structure formation, and the internal structure of the asteroids. Understanding the tectonic histories of these small rocky bodies provides insights into the dynamics of early solar system formation as well as understanding of the role of endogenic versus exogenic processes in tectonic styles of deformation. We also review Vesta as a unique planetoid in our solar system, in that a geomorphic evaluation suggests that the geological history of Vesta may have included magmatism.

2. Tectonism on Asteroids

Decades ago, linear structural features (grooves) were identified on the Martian moon Phobos in Viking orbiter imagery and interpreted to be the likely result of the large impact that formed Stickney crater [1]. Thus, the majority of the grooves are associated with an exogenic process.

The subsequent imaging of a variety of asteroids led to new models being proposed for the formation of asteroid lineaments that include both exogenic and endogenic processes. These formation models include: 1) formation by impact [2,3], 2) fabric inherited from a parent body [4], 3) down-slope scouring [5,6,7], and 4) thermal stresses [8].

Asteroid lineaments observed appear to have several different origins, and are indicative of variable interior structures. Many of the linear structures, such as those on Ida, Eros, Lutetia and Vesta, appear to be due to impact, but some lineaments have no obvious relationship to impact craters. For example, some of the linear structures on Gaspra and Eros are indicative of a fabric in a coherent asteroid inherited from a parent body, and are consistent with previous suggestions that Gaspra and Eros are fragments of larger parent bodies [9,10]. Pervasive subsurface fracturing can also be distinguished by the polygonal shapes of some craters on Mathilde [11], Eros [12,13] and Lutetia [14]. The presence of long structural features on the surfaces of some asteroids is indicative of substantial internal strength, despite low-density values that indicate high porosity. Meanwhile, lineaments on Itokawa have been associated with boulders and are consistent with the excavation of regolith by boulder movement on a "rubble pile" asteroid [7]. Vesta presents an intermediate style of tectonic deformation, with fractures and grooves similar to those observed on other asteroids, as well as large-scale graben and trough structures more characteristic of tectonics on terrestrial planet [15]. However, unlike the terrestrial planets Vesta's main stressors have been primarily exogenic (i.e. impacts) rather than internally driven [15, 16]. It is therefore clear that determining how linear features formed on these asteroids yields important information about their internal structure and strength, as well as on its nature and history.

3. Magmatism on Asteroids

Although none of the other asteroids that have been visited to date were expected to show signs of

volcanism and/or magmatism, it has long been suspected that Vesta may have undergone volcanic and/or magmatic activity at some point in its history [e.g. 17, 18]. Spectroscopic studies of Vesta [e.g. 19, 20] show that it has similar spectral signatures to the howardite–eucrite–diogenite (HED) meteorites [e.g. 21-24]. This similarity indicates that the HEDs may be vestan fragments [e.g. 22, 25]. Since the HEDs are all igneous in nature, this in turn suggests that Vesta might have experienced volcanism or magmatism.

Hypotheses of igneous intrusion on Vesta suggested that dikes could occur on Vesta, based on mathematical and petrological modeling [17]; these models indicated that both shallow and deep dikes were possible. A detailed study of the trace-element chemistry of diogenites suggests that they possibly formed as later-stage plutons injected into the eucritic vestan crust [27]. There may also be many sill-like intrusions at the base of Vesta's lithosphere [28].

The search for volcanic and magmatic features was thus a primary focus of the Dawn mission at Vesta. A comprehensive evaluation of lobate flows on Vesta yielded no unequivocal morphologic evidence of ancient volcanic activity [26]. However, some indication of magmatic processes has been identified [16]. A synthesis of tectonic, geomorphic and compositional analyses of the elongate hill Brumalia Tholus suggests that it formed as molten material utilized a subsurface fault as a conduit to travel towards Vesta's surface, intruding into and deforming the rock above it [16].

4. Summary

As a group, asteroids represent some of the earliest remnants of the early solar system. Deciphering the tectonic histories of these bodies provides insight into the complex dynamical and geological history of the inner solar system. Although currently limited by available observations, our understanding of asteroid composition and structure has grown exponentially in the last few decades, leading to improved recognition and classification of asteroid characteristics based on strength and cohesion. Impact processes dominate the tectonic styles observed on many asteroids, but there is also evidence for structure inherited from parent bodies. Vesta represents a transitional form of tectonics that reflects its internal differentiation and impact history, and observations suggest that its geologic history may have included endogenic magmatism.

As we study the icy dwarf planets of Ceres and Pluto, a better understanding the styles of tectonism, and the endogenic versus exogenic processes involved on these smaller bodies will aid in the interpretation of tectonism and volcanism on all solid bodies in the solar system.

References

[1] Thomas, P. & Veverka, J., *Icarus*, **40**, 394-405, 1979.
[2] Asphaug, E. & Melosh, H. J., *Icarus*, **101**, 144-164, 1993.
[3] Asphaug, E. et al., *Icarus*, 120, 158-184, 1996.
[4] Thomas, P. C. et al., *GRL*, **29**(10), doi: 10.1029/ 2001GL014599, 2002.
[5] Head, J. W. & Cintala, M. J., *In*: Reports of the Planetary Geology Program 1978-1979, NASA Tech. Memo., 80339, 19-21, 1979.
[6] Wilson L. & Head J. W., *LPSC XX*, 1211-1212, 1989.
[7] Sasaki, S. et al., *LPSC XXXVII*, abs. 1671, 2006.
[8] Dombard, A. J. & Freed, A. M., *GRL*, **29**(16), 65-1-65-4, 2002.
[9] Veverka, J. et al., *Icarus*, **107**, 399-411, 1994.
[10] Buczkowski, D. L. et al., *Icarus*, **193**(1), 39-52, 2008.
[11] Thomas, P. C. et al., *Icarus*, 140, 17-27, 1999.
[12] Robinson, M. S. et al., *Met. Planet. Sci*., **37**, 1651-1684, 2002.
[13] Prockter, L. et al., *Icarus*, **155**, 75-93, 2002.
[14] Thomas, N. et al., *Planet. Space Sci*., **66**, 96-124, 2012.
[15] Buczkowski, D. L. et al., *GRL*, **39**(18), L18205, 2012.
[16] Buczkowski, D.L. et al., *Icarus* doi:/10.1016/j.icarus. 2014.03.035, 2014.
[17] Wilson, L. & Keil, K., *J. Geophys. Res.*, **101**(8), 18,927-18,940, doi: 10.1029/96JE01390, 1996.
[18] Keil, K., *In*: *Asteroids III*. Univ. Arizona Press, Tucson, 573-584, 2002.
[19] McCord, T. B., et al., *Science*, **168**, 1445-1447, doi: 10.1126/science.168.3938.1445, 1970.
[20] Gaffey, M. J. 1997, *Icarus*, **127**, 130-157, doi: 10.1006/icar.1997.5680, 1997.
[21] Drake, M. J., *In*: *Asteroids*. Univ. Arizona Press, Tucson, 765–782, 1979.
[22] Drake, M. J., *Met. Planet. Sci.*, **36**(4), 501-513, doi: 10.1111/j.1945-5100.2001.tb01892.x, 2001.
[23] Consolmagno, G. J. & Drake, M. J., *Geochim. et Cosmochim. Acta*, **41**, 1271-1282, 1977.
[24] Takeda, H., *Met. Planet. Sci.*, **32**(6), 841-853, doi: 10.1111/j.1945-5100.1997.tb01574.x, 1997.
[25] Binzel, R. P. & Xu, S., *Science*, **260**, 186-191, doi: 10.1126/science.260.5105.186, 1993.
[26] Williams, D.A. *et al.*, *Planet. Space Sci.*, doi: 10.1016/j.pss.2013.06.017i, 2013.
[27] Barrat, J. A., et al., *Geochim. et Cosmochim. Acta*, **74**, 6218-6231, 2010.
[28] Wilson, L. & Keil, K., *Chemie der Erde – Geochem.*, **72**(4), 289-322, doi: 10.1016/j.chemer.2012.09.002, 2012.

EPSC Abstracts
Vol. 10, EPSC2015-432, 2015
European Planetary Science Congress 2015
© Author(s) 2015

The role of impact structures in localizing explosive volcanism on a contracting planet: Mercury

R.J. Thomas (1), D.A. Rothery (1), S.J. Conway (1) and M.Anand (1,2)
(1) Dept. of Physical Sciences, The Open University, Milton Keynes, MK7 6AA, U.K., (2) Department of Earth Sciences, The Natural History Museum, Cromwell Road, London, SW7 5BD, U.K (Rebecca.thomas@open.ac.uk)

1. Introduction

A long history of global contraction on Mercury is attested to by thousands of ridges and scarps, thought to be the surface expression of thrust faults [1]. The resulting compressive crustal stress presents an obstacle to surface volcanism on the planet, inhibiting magma ascent from depth. Nevertheless, volcanic vents and deposits indicate that explosive volcanism persisted on the planet until as recently as 1 Ga [2]. The common localization of this volcanism within impact craters and inwards of the rims of large impact basins [3] indicates that impact structures play a role in allowing volcanic eruption on this contracting body. By making a comparison with explosive volcanism within impact craters on the Moon, we investigate how ascending magma and impact structures interact on a local scale to facilitate such eruptions on Mercury. Additionally, in light of the surprisingly low number of large impact basins on Mercury [4], we investigate whether the detection of clusters of sites of explosive volcanism can provide evidence for the location of ancient impact basins that are no longer detectable morphologically.

2. Localization within impact craters

2.1 The existing lunar model

Pyroclastic deposits are commonly seen within impact craters on the Moon [e.g. 5-6], and are thought to be sourced from a shallow magmatic intrusion beneath the crater floor. It is hypothesised that ascending magma stalls in the low-density brecciated zone beneath the crater, propagates laterally to the horizontal extent of brecciation, then inflates and fractures the overlying crater floor [7]. These fractures favour magma ascent at the outer floor margins. To determine whether this is a feasible mechanism by which explosive volcanism becomes localized in impact craters on Mercury, we compared the morphology, scale and tectonic association of pyroclastic deposits and vents in 16 complex craters on Mercury and 15 on the Moon.

2.2 Results and implications

We find that host crater deformation and vent location differ significantly on the two bodies. While the floor of the host crater is fractured in all lunar cases, it is neither fractured nor deformed at sites on Mercury. Moreover, vents are commonly near the crater wall on the Moon (10 of 15 sites), but at the crater's central uplift on Mercury (14 of 16 sites).

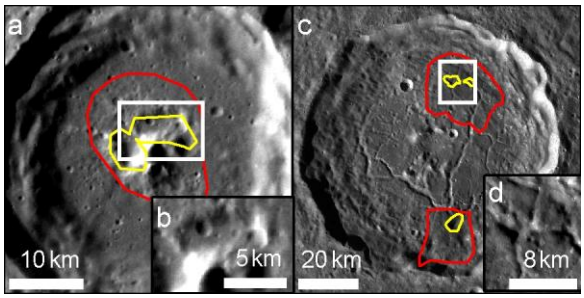

Fig. 1: Characteristic appearance of crater-hosted explosive volcanic vents (yellow outlines) and deposits (red outlines) on a. Mercury (MESSENGER NAC images, NASA/JHUAPL/ Carnegie Institute Washington) and c. the Moon (LROC WAC mosaic), with close-ups of vents, b. and d., indicated by white rectangles.

The scale of vents and deposits indicates a higher energy of eruption on Mercury than on the Moon. The maximum ballistic range (based on deposit extent) is larger at sites on Mercury (18.6 ± 1.2 km) than on the Moon (10.7 ±0.04 km). As both bodies are virtually airless but gravity is greater on Mercury, particles ejected at the same velocity will have a smaller range on Mercury. Therefore, the furthermost particles must have been ejected at considerably higher velocity on Mercury, indicative of a higher

volatile mass fraction in the erupting magma [8]. Moreover, vents are much larger on Mercury (average volume 25.0 ± 2.1 km^3 vs. 0.54 ± 0.06 km^3), consistent with more intense erosion of the conduit during higher energy eruption.

The implied high volatile mass fraction powering eruptions on Mercury suggests a period of subsurface magma storage prior to eruption, during which volatiles were concentrated in the melt by fractional crystallisation and/or remobilization of volatiles in the crust. This is supported by the presence of multiple vents at some sites, which are best explained by repeated eruption from a single local source. However, the lack of surface deformation indicates that this storage was at a greater depth than on the Moon. We propose that this results from the compressive stress in Mercury's crust, which hinders magma ascent to a level of neutral buoyancy and favours deep intrusion. On Earth, pre-existing overlying fractures are essential to allow dyke propagation to the surface in such a setting [9]. On Mercury, the common localization of explosive volcanism at the crater central uplift indicates that the deep-going, high-angle faults that are thought to bound such uplifts [10] probably play this role.

3. Explosive volcanism as evidence for ancient impact basins

Sites of explosive volcanism show conspicuous alignments in some regions of Mercury [3]. It has been proposed that the occurrence of such alignments inwards of the putative rims of the large basins Caloris and "b54" indicates that magma ascent there is favoured by the deep structures of the basins [3,11]. We compared the global distribution of sites of explosive volcanism to recently-published maps of elemental abundance [12] and crustal thickness [13] to determine whether alignments of vents occur at the margins of compositional anomalies (which could indicate excavation from depth in very large impacts) and relatively thin crust.

We observe that sites of explosive volcanism do indeed occur along the margins of regions of anomalously thin crust in several regions. One such is the compositionally-defined High-Magnesium Region (HMR), which has been proposed, on the basis of its anomalous composition and low crustal thickness, to be an ancient impact basin (Fig 2) [12]. The occurrence of multiple sites of explosive volcanism along the outer margins of this region supports the basin hypothesis.

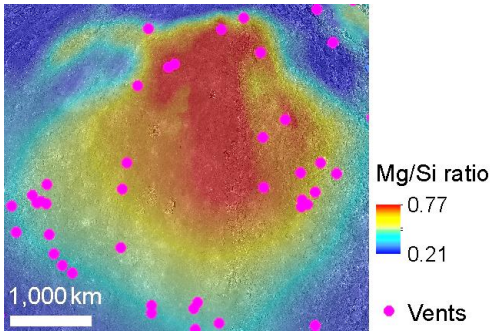

Fig. 2: Sites of explosive volcanism around the HMR. Base image: Mg/Si map [12] centred on 90.4°W, 17.9°N, superposed on MESSENGER global monochrome mosaic V9 (NASA/JHUAPL/ Carnegie Institute Washington).

6. Summary and Conclusions

- The nature of explosive volcanism within impact craters on Mercury and the Moon supports the localization of magma in the brecciated zone beneath crater floors on both bodies. However, deeper magma storage is indicated on Mercury. This is probably due to compressive stress in Mercury's crust and favours energetic eruption.
- A comparison of the distribution of sites of explosive volcanism and composition and crustal thickness data on Mercury provides supporting evidence for an ancient giant impact basin, no longer visible morphologically, in a region with an anomalously high surface Mg/Si ratio (HMR).

References

[1] Byrne, P.K. et al., *Nat. Geosci*., 7, 301-307, 2014. [2] Thomas, R.J. et al: *Geophys. Res. Lett.*, 41(17), 6084-6092, 2014. [3] Thomas, R.J. et al., *J. Geophys. Res. Planets*, 119, 22-39-2254, 2014. [4] Fassett, C.I. et al. *J. Geophys. Res.*, 117, E00L08, 2012. [5] Head, J.W. & Wilson, L. *Lunar Planet. Sci. Conf. Proc.*, 10, 2861–2897, 1979. [6] Gaddis, L. R. et al. *Lunar Planet. Inst. Sci. Conf.*, 44, 2262, 2013. [7] Schultz, P. H., *Moon*, 15, 241–273, 1976. [8] Wilson, L., J. *Volcanol. Geotherm. Res.*, 8, 297–313, 1980. [9] Chaussard, E. & Amelung, F., *Geochemistry, Geophys. Geosystems*, 15(4), 1407–1418, 2014. [10] Kenkmann, T. et al., *J. Struct. Geol.*, 62, 156–182, 2014. [11] Rothery, D.A. et al., *Earth Planet. Sci. Lett.*, vol. 385, 59–67, 2014. [12] Weider, S.Z. et al., *Earth Planet. Sci. Lett.*, 416, 109–120, 2015. [13] Mazarico, E. et al., *J. Geophys. Res. Planets*, 2014.

EPSC Abstracts
Vol. 10, EPSC2015-547, 2015
European Planetary Science Congress 2015
© Author(s) 2015

Review on material recycling in planetary bodies

K.Kurita (1), D. Shoji (2), H.Ichikawa (3) and S,Omori(4)

(1) ERI, The Univ. of Tokyo,Tokyo, Japan, (2) DLR, Berlin,Germany, (3) GRC,Ehime University,Matsuyama,Japan, (4) Open Univ. Japan,Chiba,Japan

(corresponding address kurikuri@eri.u-tokyo.ac.jp / Fax: +81-25841-0796)

Abstract

As a basic process to drive material recycling without the plate tectonics in planetary bodies we propose a delamination process in the surface layer. Particularly we focus on the compositional delamination. In the silicate system the basaltic surface crust is produced by melting, which can transform higher density layer at depth. In icy bodies infall of ice/rock mixture can form higher density surface layer. In either situation the density reversal of the surface is expected to develop, which can drive delamination of bottom of the surface layer. We will review various styles of delamination in wide ranges of planetary/satellite systems.

1. Introduction

In planetary/satellite systems where the plate tectonics is not working thermal plumes contribute material transport from the inside and differentiations through induced volcanism. To ensure material recycling to the interior only possible style would be overturn/delamination of the surface crust. Since this process is principally Rayleigh-Taylor Instability, it requires development of density reversal of the surface layer. In this presentation we focus on the delamination as a basic style of mantle dynamics without the plane tectonics and review various styles of the delamination in wide ranges of planetary/satellite systems.

2. Two models

There are two origins for the development of density reversal of the surface: thermal and compositional origins, which will be driving factors for the delamination. In the thermal origin model, the surface boundary layer due to the planetary secular cooling becomes denser because of lower temperature. Since the uppermost layer is expected to be strong the intermediate layer between the surface and the interior could deform to be delaminated from the upper[1]. But this model is essentially same as the convective instability of the boundary layer and no compositional differentiation is involved so that the recycling can not affect the compositional evolution. In the compositional origin model the basalt formed by melting of the silicate mantle can transform to eclogite at depth, which could be denser than the mantle. Growing this layer can induce delamination. After first explicit description by Kay and Kay [2] this process has been widely considered in the orogenic tectonics in the Earth. In Venus importance of basalt-eclogite transition has been well recognized in 1990s such as [3] and [4] the role as a recycling process has only been incorporated since Dupeyrat et al 1999. Since the basalt-eclogite transition is induced at high pressures, a large planetary body is required. The exception is Mars, where iron-rich basaltic crust can transform to eclogite at relatively low pressure and thus induced delamination is highly plausible[6]. The model is extended to the case of super-Earth [7]
Similar process is incorporated in the evolution models of icy bodies [8] and Ceres [9] though the origin of density anomaly is exogenetic.

3. Some problems

There exist several problems to evaluate compositional delamination process properly. The most significant one, which is stated in [10] is the higher strength of eclogite comparing to the surrounding materials. This could resist deformation and detachment from the upper layer. This situation makes quite difficult to evaluate time scale of the process. In the current numerical treatments incorporation of high-strength behavior such as the

fracturing process is difficult. Role of water in reduction of the strength and phase transition-induced weakening along the boundary may be important.

4. Planetary volcanism as observational constraints

Since the delamination itself is going on well below the surface it is quite difficult to trace and characterize by observable data ;the planetary remote sensing explorations. Here we suggest a volcanism as a surface manifestation of the delamination. In the Earth there exist many examples of delamination-induced volcanism[11]. The delamination could induce adiabatic rise of the mantle as a compensating flow. If the mantles temperature is close to the solidus it can easily melt during the ascent, which can appear as volcanoes at the surface. The volcanism such as at Colorado Plateau[12] and [13]Carpathia is proposed as a site of delamination-induced volcanism. We propose to explore characterization of volcanism in relation to other features such as gravity field in the planetary exploration data as well as extensive comparison with terrestrial examples for the future works.

References

[1] Bird, P.:JGRB 84,7561,1979.

[2] Kay, R. and Kay, S.: Tectonophysics 219,177,1993.

[3] Namiki, N. and S.Solomon.: JGRE 91,15025,1993.

[4] Dupeyrat, L. and C.Sotin:PSS 43,909,1995.

[5] Dupeyrat, L. et al: JGRE 104,27163, 1999.

[6] Kurita, K. et al EPSC 2013

[7] Shoji, D. and K.Kurita: PSS 109-110,38,2015.

[8] Rubin, M. et al: Icarus 236,122,2014.

[9] Shoji,D. and K.Kurita: JGRE 119,2014.

[10] Nimmo, F. and D.Mckenzie: Ann.Rev.Eart Planet. Sci.,26,23,1998

[11] Ducea, M.:Geology 39,119,2011

[12] Manley, C. et al: Geology 28,811,2000.

[13] Ismail-Zadeh et al. :GJInt. 168,1276,2007.

EPSC Abstracts
Vol. 10, EPSC2015-909, 2015
European Planetary Science Congress 2015
© Author(s) 2015

Planet-wide cessation of major effusive volcanism on Mercury

Paul K. Byrne (1,2), Lillian R. Ostrach (3), Brett W. Denevi (4), Clark R. Chapman (5), Caleb I. Fassett (6), Jennifer L. Whitten (7), Christian Klimczak (8,2), Erwan Mazarico (3), Steven A. Hauck, II (9), James W. Head (10), and Sean C. Solomon (11,2). (1) Lunar and Planetary Institute, Universities Space Research Association, Houston, TX 77058, USA (byrne@lpi.usra.edu); (2) Department of Terrestrial Magnetism, Carnegie Institution of Washington, Washington, DC 20015, USA; (3) Solar System Exploration Division, NASA Goddard Space Flight Center, MD 20771, USA; (4) The Johns Hopkins University Applied Physics Laboratory, Laurel, MD 20723, USA; (5) Department of Space Studies, Southwest Research Institute, Boulder, CO 80302, USA; (6) Department of Astronomy, Mount Holyoke College, South Hadley, MA 01075, USA; (7) Center for Earth and Planetary Studies, Smithsonian Institution, Washington, DC 20013, USA; (8) Department of Geology, University of Georgia, Athens, GA 30602, USA; (9) Department of Earth, Environmental, and Planetary Sciences, Case Western Reserve University, Cleveland, OH 44106, USA; (10) Department of Earth, Environmental and Planetary Sciences, Brown University, Providence, RI 02912, USA; (11) Lamont-Doherty Earth Observatory, Columbia University, Palisades, NY 10964, USA.

1. Introduction

The importance of volcanism for the formation of Mercury's crust was affirmed by MESSENGER observations of the planet acquired during its three flybys in 2008–10. Smooth plains units were identified across Mercury, and embayment relations, spectral contrast with surrounding terrain, and morphologic characteristics indicated that most of these plains are volcanic in origin [e.g., 1].

Orbital data have allowed the global distribution of these plains units to be characterized [2]. The largest such deposits are located in the northern hemisphere and include the extensive northern plains (NP) and the Caloris interior and exterior plains (with the latter likely including basin ejecta material). Crater size–frequency analyses have shown that both the NP and the Caloris interior deposits were emplaced, within statistical error, around 3.8 Ga [2–6], for any of the published chronology models for Mercury [e.g., 7]. The areal densities of impact craters (for a given range of crater diameters) for other smooth plains deposits across Mercury are comparable to those for the NP and Caloris plains, implying that these other units are similar in age [2,4,6,8].

To test whether this age marked a period of globally distributed volcanic resurfacing on Mercury, we determined crater size–frequency distributions for six additional smooth plains units, primarily in the planet's southern hemisphere, interpreted as volcanic.

2. Crater Spatial Density Analysis

Each of these six sites hosts two populations of impact craters—one that postdates plains emplacement, and one that consists of partially to nearly filled craters that predate the plains. This latter population indicates that, in each case, considerable time elapsed between formation of the underlying basement and the plains.

The largest region of smooth plains at high southern latitudes we investigated is situated proximal to (and is named for) the Alver and Disney impact craters [9]. Farther west, a smaller patch of smooth plains is not obviously associated with an impact structure and so is termed here the "southern plains." The largest unit of those we examined is located at mid-latitudes in the southern hemisphere and is superposed by the 80-km-diameter Debussy impact crater. In the western hemisphere, smooth plains units within the Beethoven and Tolstoj basins constitute two additional sites; earlier studies have also reported crater density data for Beethoven [2,8]. The northernmost site encompasses, but extends far beyond, the 168-km-diameter Faulkner basin, for which earlier crater density data also exist [2].

3. Results

We give in **Table 1** our crater density measurements for each site in terms of $N(10)$, the number of craters 10 km in diameter or greater per 10^6 km^2 [e.g., 6]. This approach has the benefit of allowing direct comparison of disparate sites without the use of a particular model production function. (We give confidence intervals of ± one standard deviation, taken to equal the square root of the number of craters normalized to an area of 10^6 km^2 [e.g., 4]).

The six sites fall into two groups by $N(10)$, with higher counts (within error) for the plains at Alver/Disney, Beethoven, and Debussy than for those at Faulkner, the southern plains, and Tolstoj. However, the plains at Faulkner host a greater

number of secondary impact craters than at any of the other sites; our efforts to exclude secondaries at Faulkner from our count, on the basis of their occurrence in chains and clusters, may have contributed additional uncertainty to the *N*(10) value we calculated for that site.

Table 1: Smooth plains *N*(10) values from this study

Site	*N*(10)	Area (km^2)
Alver/Disney	132 ± 20	3.4×10^5
Beethoven	100 ± 18	3.0×10^5
Debussy	161 ± 20	4.2×10^5
Faulkner	39 ± 10	3.6×10^5
Southern plains	53 ± 27	7.5×10^4
Tolstoj	45 ± 20	1.1×10^5

Additionally, the southern plains and Tolstoj units are substantially smaller than, and so their *N*(10) values may not be as statistically robust as those for, the other units in this work. Nonetheless, the collective span of *N*(10) we give here is comparable to previously reported values for these and other volcanic smooth plains, and substantially lower than the range found for several intercrater plains units (**Table 2**).

Table 2: Earlier *N*(10) values for plains units

Site	*N*(10)	Ref.
Beethoven	82 ± 19 | 77 ± 24	[2] | [8]
Caloris interior plains	58 ± 13 | 75 ± 7	[2] | [4]
Caloris exterior plains	91 ± 16	[2]
Faulkner	58 ± 18	[2]
Northern plains	67 ± 4	[6]
Rembrandt	103 ± 19 | 110 ± 23	[2] | [8]
Rudaki	51 ± 23	[2]
Intercrater plains	154 ± 34 → 370 ± 53	[8]

Importantly, although small deposits in Rachmaninoff and Raditladi basins may be as young as 1 Ga [10,11], we have yet to identify widespread (e.g., >1 × 10^5 km^2) effusive volcanic deposits anywhere on Mercury with resolvably lower *N*(10) values than those we report.

4. Planet-wide cessation of major effusive volcanism

It has long been noted that many volcanic smooth plains units on Mercury, including the Caloris interior plains and those in Beethoven, Rembrandt, and Tolstoj, are situated within pre-existing impact basins and craters [e.g., 9]. So, too, are many smaller deposits across the planet, at least some of which are likely volcanic. This collocation of many of the youngest effusive volcanic units on Mercury with impact structures is consistent with predictions for a planet undergoing contraction from secular interior cooling [12].

Global contraction induced a state of net horizontal compression in Mercury's lithosphere, inhibiting the vertical ascent and eruption of magma [13]. However, the impact process would not only have deposited impact heat at depth, but would have removed overburden, fractured the lithosphere, and reset stresses locally—making impact structures prime sites for late-stage eruptions in a tectonic regime otherwise generally unfavorable to extrusive activity.

The volcanic smooth plains across Mercury may reflect a peak in magma generation [e.g., 14] or instead may simply have arisen from the rapidly waning impact flux toward the end of the late heavy bombardment of the inner Solar System [15]. Nonetheless, global contraction likely was underway by this time [16] and may, in and of itself, account for the absence of resolvably younger, widespread effusive volcanic deposits on Mercury [13]. If the rate of magma production after the onset of global contraction did not diminish in step with the rate of effusive resurfacing, the ratio of intrusive to extrusive material may be greater for the innermost planet than for bodies with longer histories of effusive surface volcanism [e.g., 17].

References

[1] Head J. W. et al. (2008) *Science*, *321*, 69–72. [2] Denevi B. W. et al. (2013) *JGR Planets*, *118*, 891–907. [3] Head J. W. et al. (2011) *Science*, *333*, 1853–1856. [4] Fassett C. I. et al. (2009) *EPSL*, *285*, 297–308. [5] Strom R. G. et al. (2011) *PSS*, *59*, 1960–1967. [6] Ostrach L. R. et al. (2015) *Icarus*, *250*, 602–622. [7] Le Feuvre M. & Wieczorek M. A. (2011) *Icarus*, *214*, 1–20. [8] Whitten J. L. et al. (2014) *Icarus*, 241, 97–113. [9] Fassett, C. I. et al. (2012) *JGR*, *117*, E00L08. [10] Prockter L. M. et al. (2010) *Science*, *329*, 668–671. [11] Marchi S. et al. (2011) PSS, 59, 1968–1980. [12] Solomon, S. C. (1978) *GRL*, *5*, 461–464. [13] Wilson L. & Head J. W. (2008) *GRL*, *35*, L23205. [14] Michel N. C. et al. (2013) *JGR Planets*, *118*, 1033–1044. [15] Marchi S. et al. (2013) *Nature*, *499*, 59–61. [16] Banks M. E. (2014) *LPS 45*, abstract 2722. [17] Greeley R. & Schneid B. D. (1991) *Science*, *254*, 996–998.

EPSC Abstracts
Vol. 10, EPSC2015-915, 2015
European Planetary Science Congress 2015
© Author(s) 2015

Putative volcanic landforms on Ceres

T. Platz (1), A. Nathues (1), M. Hoffmann (1), M. Schäfer (1), D.A. Williams (2), S.C. Mest (3), D.A. Crown (3), M.V. Sykes (3), J.-Y. Li (3), T. Kneissl (4), N. Schmedemann (4), O. Ruesch (5), H. Hiesinger (6), H. Sizemore (3), I. Büttner (1), P. Gutierrez-Marques (1), J. Ripken (1), C.A. Raymond (7), C.T. Russell (8), T. Schäfer (1), G.S. Thangjam (1)

(1) Max Planck Institute for Solar System Research, Göttingen, Germany (platz@mps.mpg.de); (2) Arizona State University, Tempe, USA; (3) Planetary Science Institute, Tucson, USA; (4) Freie Universität Berlin, Berlin, Germany; (5) NASA Goddard Space Flight Center, Greenbelt, USA; (6) University of Muenster, Muenster, Germany; (7) Jet Propulsion Laboratory, California Institute of Technology, Pasadena, USA; (8) University of California, Los Angeles, USA.

Abstract

In the first RC2 and OpNav7 images of Dawn's approach at Ceres a number of intriguing landforms are observed, which potentially have formed by volcanic activity. These and subsequently discovered features will be monitored and validated on higher resolution datasets as acquired later in 2015.

1. Introduction

On March 6, 2015 the Dawn spacecraft was captured by Ceres' gravity field. Several optical navigation (OpNav) and rotation characterization (RC) observations were acquired during approach phase by the Framing Camera (FC) [1, 2]. In this preliminary study we used images of RC2 and OpNav7 campaigns taken on February 19, 2015 and April 15, 2015, respectively. We present and describe landforms that may have formed by volcanism. Pending further high-resolution image surveys, tentative comments are made regarding the nature of volcanism.

2. Data and methods

At the Max Planck Institute for Solar System Research RC2 and OpNav7 images have been processed and were resampled to resolutions of 2 km/px and 1.5 km/px, respectively. Of particular interest are those images acquired at low solar elevation (i.e., high incidence angle). Individual images are analyzed using USGS ISIS and ESRI's GIS environments. Elevation data are derived from the shape model provided by Nickolaos Mastrodemos (JPL).

3. Morphology

The surface of Ceres shows a variety of landforms including impact craters and basins, lineaments, and smooth and rough textured terrains. Current geological activity is manifested by bright spots, where presumably water sublimates [3].

At low solar elevation, a number of intriguing positive relief features are observed resembling cones and/or low-relief shields and domes. Three examples are provided below.

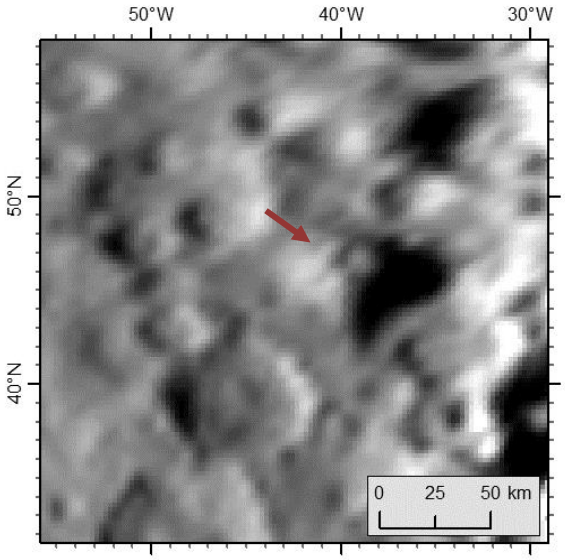

Figure 1: Site 1 – isolated, up to 4 km high mountain.

At 47.5°N/319.3°E[1] (site 1) an isolated mountain with a basal diameter of ~40 km and a height of up to 4 km is observed (height estimate is based on the shadow cast method [4, 5]). Near the summit a crater exits (Fig. 1). At site 2 (15.8°S/5.8°E[1]) two landforms are observed. At the lower centre a c.50-

km diameter flat-topped dome is present. About 50 km to the north, a broad S-shaped, flat-topped ridge with steep margins is observed (Fig. 2). Site 3 shows the largest impact basin observed so far on Ceres. The c.273-km diameter basin has a pentagonal outline with the northwestern rim being partially buried and dissected (Fig. 3). The basin interior and exterior (particularly to the west) is characterised by smooth-textured infill. The basin centre is marked by a c.26-km diameter pit. The basin floor shows a high-relief with the lowest point at the centre located approx. 5-6 km below elevated portions of floor materials. At the western rim a set of five small domes or cones is present.

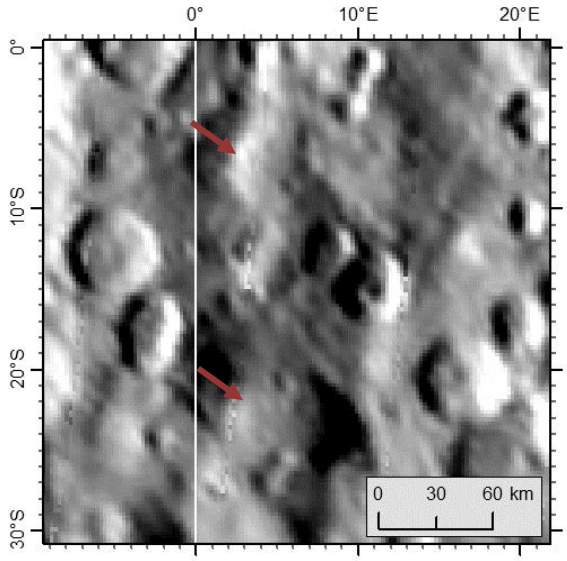

Figure 2: Site 2 – flat-topped dome (lower arrow) and ridge (upper arrow) near the prime meridian (white vertical line).

4. Preliminary conclusions

Ceres experienced a complex resurfacing history indicated by smooth-textured terrains in the vicinity of the c.273-km diameter basin. These smooth terrains lack mid-sized impact craters when compared to the overall crater population suggesting portions of this population were erased or buried. Though impact-related resurfacing could be the primary process, observed landforms, however, also suggest an endogenous process. At present, available imagery cannot resolve detailed morphological features, and therefore, cannot clearly link described landforms to a volcanic origin. The overall morphometry (i.e., height and slopes) of landforms, however, points to an endogenous formational process. If a volcanic origin is substantiated following higher resolution Survey, HAMO, and LAMO image analyses, the type of volcanism—silicate/carbonaceous, mud and/or cryovolcanism—need to be assessed. At the EPSC we present new data and results from Survey and HAMO campaigns.

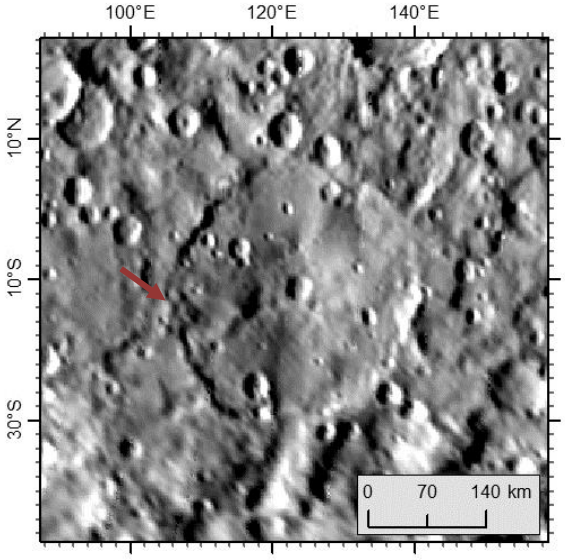

Figure 3: Site 3 – large infilled basin. Arrow points to a group of cones.

5. References

[1] Russell, C.T., and Raymond, C.A., 2012, Space Sci. Rev., 163, 3–23. [2] Sierks, H. et al., Space Sci. Rev., 163, 263–328, 2012. [3] Nathues, A. et al. EPSC 2015, #60115. [4] Pike, R.J., Geophys. Res. Lett., 1, 291–294, 1974. [5] Pike, R.J., 11th Proc. Lunar Planet. Sci. Conf., 2159–2189, 1980.

[1] provisional coordinates